Kybernetika

Chengcheng Wang; Xianglei Jia; Chengdi Xiang; Yingying Han
Disturbance observer-based robust control for a class of uncertain nonlinear systems

*Kybernetika*, Vol. 62 (2026), No. 4, 561–583

Persistent URL: http://dml.cz/dmlcz/153774

**Terms of use:**

© Institute of Information Theory and Automation AS CR, 2026

Institute of Mathematics of the Czech Academy of Sciences provides access to digitized documents strictly for personal use. Each copy of any part of this document must contain these *Terms of use*.




This document has been digitized, optimized for electronic delivery and stamped with digital signature within the project *DML-CZ: The Czech Digital Mathematics Library* http://dml.cz

KYBERNETIKA — VOLUME *62* (2026), NUMBER 4, PAGES 561–583

# DISTURBANCE OBSERVER-BASED ROBUST CONTROL FOR A CLASS OF UNCERTAIN NONLINEAR SYSTEMS

Chengcheng Wang, Xianglei Jia, Chengdi Xiang and Yingying Han

This paper addresses the global output regulation problem for a class of strict-feedback systems subject to unknown nonlinearities and mismatched disturbances. A composite robust control strategy based on backstepping, high-gain scaling and disturbance observers is developed. In particular, unknown mismatched nonlinearities are suppressed by introducing high-gain scaling, and mismatched disturbances are compensated for by improved disturbance observers. Rigorous Lyapunov analysis guarantees the global stability of the closed-loop system and the achievement of output regulation. A key advantage of the proposed controller is that it does not rely on specific models of nonlinearities, thus ensuring strong robustness to model uncertainties. Finally, simulation results are provided to validate the effectiveness of the proposed method.

*Keywords:* backstepping control, disturbance observers, high-gain scaling, nonlinear systems

*Classification:* 93C10, 93C73, 93D05

## 1. INTRODUCTION

In modern industrial applications such as robotic manipulators and power systems, parameter uncertainties and external disturbances are ubiquitous, which seriously undermine the stability and control accuracy of closed-loop systems. Consequently, building on classical nonlinear adaptive control [8], the development of advanced robust control strategies for such systems has attracted significant attention [3, 6, 22]. Traditional approaches mostly adopted sliding mode control [4] or backstepping [21], but faced significant design difficulties when dealing with mismatched disturbances, as pointed out in [2, 16].

To address this issue, disturbance observer-based control (DOBC) [5, 9, 10, 13, 24, 29] has gained considerable popularity due to its active compensation capability, and by combining with robust control, it has become an effective strategy for addressing mismatched disturbance problems [12, 17, 18, 25]. For instance, Ref. [18] proposes a disturbance observer-based nonsingular terminal sliding mode control scheme for the simultaneous suppression of matched and mismatched uncertainties. Ref. [17] addressed the problems of stability and disturbance rejection for fractional-order systems by proposing

DOI: 10.14736/kyb-2026-4-0561

a composite scheme that combines the disturbance observer with fractional-order sliding mode. Moreover, Ref. [25] proposed a finite-time sliding mode control method based on a disturbance observer to enhance the system performance in the presence of mismatched disturbances. Although the aforementioned methods are highly effective in suppressing external disturbances, they often assume that the nominal nonlinear functions of the system are known. To further address the modeling challenge of unknown nonlinear functions within the system, intelligent control strategies incorporating neural networks or fuzzy logic systems have emerged as mainstream approaches to resolving model uncertainties [7, 11, 20, 23, 27]. However, despite their excellent approximation performance, intelligent control methods can only ensure the system to achieve semi-global stability, which limits their application in engineering scenarios with high reliability requirements.

To circumvent this limitation and achieve global stability without relying on function approximators, high-gain control or homogeneous domination methods provide an alternative approach without relying on specific model information [1, 14, 19, 26, 30, 31]. The central tenet of this category of approaches lies in quelling the impacts of unknown nonlinear terms via the incorporation of a high-gain adjustment mechanism. They have been extensively adopted to tackle a variety of output feedback stabilization challenges, and striking achievements have been attained in specific nonlinear systems, such as stochastic feedforward systems [15] and high-order nonlinear systems [28]. However, most existing high-gain control methods focus on addressing the internal nonlinearities of the system. How to organically integrate high-gain technology with the active disturbance rejection capability of disturbance observers, thereby simultaneously achieving efficient suppression of mismatched non-vanishing disturbances without relying on accurate model information, remains a pressing challenge to be addressed.

A composite robust control strategy, incorporating a high-gain disturbance observer, is developed in this work to address the global output regulation problem for a class of strict-feedback systems subject to both unknown nonlinearities and mismatched non-vanishing disturbances. This paper's primary contributions are threefold:

- The integration of high-gain scaling empowers the proposed observer to deliver effective estimation and compensation of mismatched disturbances under the relaxed assumption of linearly bounded nonlinearities, thereby eliminating the dependency on precise model information that constrains conventional designs.

- It abandons the reliance of intelligent control methods such as neural networks on universal function approximators and cumbersome online learning processes, directly dominates unknown nonlinear terms using a concise high-gain linear structure, effectively overcomes the curse of dimensionality, significantly reduces the computational burden of the algorithm, and is more conducive to real-time engineering implementation.

- Rigorous Lyapunov analysis demonstrates that the closed-loop system achieves global stability within the proposed unified high-gain-disturbance-observer framework, even when contending with partially unknown nonlinearities and mismatched disturbances.

**Notations.** $\mathbb{R}$ is the set of real numbers; $\mathbb{R}^n$ is the set of $n$-dimensional real vectors;

$\mathbb{R}^{n\times m}$ is the set of $n$-by-$m$ real matrices; $\min\{\cdot\}$ denotes the minimum value; $\|\cdot\|$ denotes the Euclidean norm or the spectral norm.

## 2. PRELIMINARIES

### 2.1. Problem formulation

Consider the strict-feedback nonlinear system with mismatched non-vanishing disturbances, described by

$$\begin{aligned} \dot{x}_1 &= x_2 + f_1(x_1) + d_1(t), \\ \dot{x}_2 &= x_3 + f_2(x_1, x_2) + d_2(t), \\ &\vdots \\ \dot{x}_n &= u + f_n(x_1, x_2, \ldots, x_n) + d_n(t), \\ y &= x_1, \end{aligned} \tag{1}$$

where $x = [x_1, \ldots, x_n]^T \in \mathbb{R}^n$, $u \in \mathbb{R}$, and $y \in \mathbb{R}$ are the system state, input, and output, respectively. $d_i(t)$ and $f_i(x_1, \ldots, x_i)$ represent lumped disturbances and unknown nonlinear functions, for $i = 1, \ldots, n$.

The development of the control scheme relies on the following assumptions.

**Assumption 2.1.** The uncertain nonlinear functions satisfy the following linear growth condition, and there exist positive constants $\gamma_i$ such that

$$|f_i| \le \gamma_i(|x_1| + |x_2| + \cdots + |x_i|). \tag{2}$$

**Assumption 2.2.** There exist positive constants $\theta_1$ and $\theta_2$ that bound the external disturbances and their first derivatives. Formally, for all $i = 1, ..., n$, we have

$$|d_i(t)| \le \theta_1, \quad |\dot{d}_i(t)| \le \theta_2. \tag{3}$$

**Remark 2.3.** Assumption 2.1 requires the unknown nonlinearities $f_i$ to satisfy a global linear growth condition, meaning their growth rate is bounded by a linear combination of the system states. This relatively mild requirement makes the proposed theory applicable to a broad class of nonlinear systems. While this condition is standard in the high-gain control literature, it does impose a limitation when the system exhibits superlinear growth (e. g., $x^2$ or higher powers) over a global domain. However, for many physical systems operating within a bounded region, a local linear bound can often be established, making the method practically viable. Moreover, the constants $\gamma_i$ in (2) directly influence the magnitude of the lumped uncertainty bound $\kappa$ derived in (49): larger $\gamma_i$ lead to a larger $\kappa$, which in turn necessitates a larger gain $L$ to ensure the negative definiteness of $\dot{V}_n$ as required in (52). Hence, $\gamma_i$ quantitatively captures the trade-off between the severity of system uncertainty and the required control effort.

**Remark 2.4.** Assumption 2.2 requires bounded disturbances and their first derivatives, a common and justifiable premise in disturbance observer-based control designs. For example, it is widely adopted in the designs presented in [5, 9, 10]. The underlying rationale lies in the emergence of disturbance derivative terms within the dynamic equation of observer error, with their boundedness proving pivotal to guaranteeing the error system's stability.

### 2.2. Key lemmas

To facilitate understanding, several preliminary results to be employed subsequently are presented below. Consider the system detailed below

$$\dot{x} = \delta(t, x, u),\ x \in \mathbb{R}^n,\ u \in \mathbb{R}^m. \tag{4}$$

**Lemma 2.5.** (Sun et al. [24]) Consider a continuously differentiable function $V : [0, \infty) \times \mathbb{R}^n \to \mathbb{R}$. If $V$ satisfies the inequalities

$$\alpha_1(\|x\|) \leq V(t, x) \leq \alpha_2(\|x\|),$$

$$\frac{\partial V}{\partial t} + \frac{\partial V}{\partial x}\delta(t, x, u) \leq -G_3(x),\ \forall \|x\| \geq \vartheta(\|u\|) > 0,$$

for all $(t, x, u) \in [0, \infty) \times \mathbb{R}^n \times \mathbb{R}^m$, where $\alpha_1$ and $\alpha_2$ are class $\mathcal{K}_\infty$ functions, $\vartheta$ is a class $\mathcal{K}$ function, and $G_3(x)$ is a continuous positive definite function on $\mathbb{R}^n$. Then, system (4) is input-to-state stable (ISS).

**Lemma 2.6.** (Sun et al. [24]) If the following conditions are satisfied

- system (4) is globally ISS,
- $\lim_{t\to\infty} u = 0$,

then the states of system (4) will converge to zero asymptotically, i. e., $\lim_{t\to\infty} x = 0$.

## 3. CONTROLLER DESIGN

### 3.1. Disturbance observer design

A high-gain scaling transformation is introduced as

$$z_i = \frac{x_i}{L^i}, \tag{5}$$

where $L > 1$ is a scaling gain to be designed. Under this transformation, system (1) becomes

$$\begin{aligned} \dot{z}_i &= L z_{i+1} + \frac{f_i}{L^i} + L\bar{d}_i, \\ \dot{z}_n &= \frac{u}{L^n} + \frac{f_n}{L^n} + L\bar{d}_n, \\ y &= L z_1, \end{aligned} \tag{6}$$

where $\bar{d}_i = d_i/L^{i+1}$ denotes the scaled disturbance.

**Remark 3.1.** Coordinate Transformation (5) constitutes the linchpin of the high-gain control scheme put forward herein. It transforms the original system (1) to the $z$-coordinate system (6), such that the unknown nonlinear terms become $f_i/L^i$. As analyzed in subsequent equations (40) – (49), although $f_i$ grows with $L^k$, the $1/L^i$ term ensures that $f_i/L^i$ can ultimately be linearly bounded by $z$-coordinates (i. e., $s_j$ and $\tilde{d}_j$), with its bound $\kappa$ independent of $L$. This allows us to increase $L$ to enhance the control gain, making it ultimately dominate this fixed uncertainty bound $\kappa$, thus ensuring the stability of the system without knowing $f_i$ at all.

The disturbance observer is designed following the framework in [24]. For each $i = 1, ..., n$, it is constructed as

$$\begin{array}{rcl} \hat{d}_i & = & \lambda_i(z_i - p_i), \\ \dot{p}_i & = & Lz_{i+1} + L\hat{d}_i, \end{array} \tag{7}$$

where $\lambda_i > 0$ is a design constant, and the relationship $Lz_{n+1} = u/L^n$ holds by definition. Substituting (6) into (7) yields the disturbance estimation:

$$\dot{\hat{d}}_i = \lambda_i \left( \frac{f_i}{L^i} + L\tilde{d}_i \right). \tag{8}$$

Then, the disturbance estimation error system is characterized as

$$\dot{\tilde{d}}_i = \dot{\bar{d}}_i - \lambda_i L\tilde{d}_i - \lambda_i \frac{f_i}{L^i}, \tag{9}$$

where $\tilde{d}_i = \bar{d}_i - \hat{d}_i$.

### 3.2. Composite controller design

The controller design follows a two-step robust strategy. First, the unknown nonlinear functions $f_i$ are neglected, and a basic composite controller is designed for the nominal system (10). Subsequently, Section 4 rigorously proves that, by virtue of the high gain $L$, this same controller also ensures the uniform boundedness of the complete system that includes $f_i$.

$$\left\{ \begin{array}{rcl} \dot{z}_i & = & Lz_{i+1} + L\bar{d}_i, \\ \dot{\tilde{d}}_i & = & \dot{\bar{d}}_i - \lambda_i L\tilde{d}_i, \\ \dot{\hat{d}}_i & = & \lambda_i L\tilde{d}_i. \end{array} \right. \tag{10}$$

A recursive design procedure is now applied to the nominal system (10).

`Step 1:` Consider a Lyapunov function as

$$V_1 = \frac{1}{2}s_1^2 + \frac{1}{2}\tilde{d}_1^2, \tag{11}$$

in which $s_1 = z_1$. Computing the derivative of both sides of (11) results in

$$\begin{array}{rcl} \dot{V}_1 & = & s_1(Lz_2 + L\bar{d}_1) - \lambda_1 L\tilde{d}_1^2 + \tilde{d}_1\dot{\tilde{d}}_1 \\ & = & -\lambda_1 L\tilde{d}_1^2 + Ls_1z_2^* + Ls_1(z_2 - z_2^*) + Ls_1\bar{d}_1 + \tilde{d}_1\dot{\tilde{d}}_1. \end{array} \tag{12}$$

Employing the disturbance estimate $\hat{d}_1$ outlined in equation (7), the virtual control law $z_2^*$ is constructed as

$$z_2^* = -\varphi_1 s_1 - \hat{d}_1, \tag{13}$$

where $k_1 > 0$, $\varepsilon_1 > 0$, and $\varphi_1 = k_1 + \frac{1}{4\varepsilon_1}$. Substituting (13) into (12) yields

$$\begin{aligned} \dot{V}_1 &= -L\left(k_1 + \tfrac{1}{4\varepsilon_1}\right) s_1^2 - \lambda_1 L\tilde{d}_1^2 + Ls_1 s_2 + Ls_1\tilde{d}_1 + \tilde{d}_1\dot{\tilde{d}}_1 \\ &\leq -L\left(k_1 + \tfrac{1}{4\varepsilon_1}\right) s_1^2 - \lambda_1 L\tilde{d}_1^2 + Ls_1 s_2 + L\tfrac{1}{4\varepsilon_1} s_1^2 + L\varepsilon_1\tilde{d}_1^2 + \tilde{d}_1\dot{\tilde{d}}_1 \\ &= -Lk_1 s_1^2 - L(\lambda_1 - \varepsilon_1)\tilde{d}_1^2 + Ls_1 s_2 + \tilde{d}_1\dot{\tilde{d}}_1, \end{aligned} \tag{14}$$

where $s_2 = z_2 - z_2^*$.

`Step 2:` Consider a Lyapunov function as

$$V_2 = V_1 + \frac{1}{2}s_2^2 + \frac{1}{2}\tilde{d}_2^2. \tag{15}$$

Differentiating (15) yields

$$\begin{aligned} \dot{V}_2 \leq\ & -Lk_1 s_1^2 - L(\lambda_1 - \varepsilon_1)\tilde{d}_1^2 + Ls_1 s_2 \\ & + s_2\left(Lz_3 + L\bar{d}_2 - \tfrac{\partial z_2^*}{\partial s_1}(Lz_2 + L\bar{d}_1) - \tfrac{\partial z_2^*}{\partial \hat{d}_1}\lambda_1 L\tilde{d}_1\right) \\ & - \lambda_2 L\tilde{d}_2^2 + \tilde{d}_2\dot{\tilde{d}}_2 + \tilde{d}_1\dot{\tilde{d}}_1 \\ =\ & -Lk_1 s_1^2 - L(\lambda_1 - \varepsilon_1)\tilde{d}_1^2 - \lambda_2 L\tilde{d}_2^2 + Ls_1 s_2 + Ls_2 z_3^* + Ls_2(z_3 - z_3^*) \\ & - s_2\tfrac{\partial z_2^*}{\partial s_1}Lz_2 + s_2\left(L\bar{d}_2 - \tfrac{\partial z_2^*}{\partial s_1}L\bar{d}_1 - \tfrac{\partial z_2^*}{\partial \hat{d}_1}\lambda_1 L\tilde{d}_1\right) + \tilde{d}_2\dot{\tilde{d}}_2 + \tilde{d}_1\dot{\tilde{d}}_1. \end{aligned} \tag{16}$$

In light of the disturbance estimations $\hat{d}_1$ and $\hat{d}_2$, the virtual control law $z_3^*$ is constructed as

$$z_3^* = -s_1 - (\varphi_2 + \hat{c}_2)\, s_2 - \hat{d}_2 + \frac{\partial z_2^*}{\partial s_1}(\hat{d}_1 + z_2), \tag{17}$$

where $k_2 > 0$, $\varepsilon_2 > 0$, $\varphi_2 = k_2 + \frac{1}{4\varepsilon_2}$ and $\hat{c}_2 = \frac{1}{4\varepsilon_1}\left(\frac{\partial z_2^*}{\partial s_1} + \frac{\partial z_2^*}{\partial \hat{d}_1}\lambda_1\right)^2$.

Substituting (17) into (16) yields

$$\begin{aligned} \dot{V}_2 =\ & -Lk_1 s_1^2 - L(\lambda_1 - \varepsilon_1)\tilde{d}_1^2 - L\left(k_2 + \tfrac{1}{4\varepsilon_2} + \hat{c}_2\right) s_2^2 - \lambda_2 L\tilde{d}_2^2 \\ & + Ls_2(z_3 - z_3^*) + Ls_2\tilde{d}_2 - Ls_2\left(\tfrac{\partial z_2^*}{\partial s_1} + \tfrac{\partial z_2^*}{\partial \hat{d}_1}\lambda_1\right)\tilde{d}_1 + \tilde{d}_2\dot{\tilde{d}}_2 + \tilde{d}_1\dot{\tilde{d}}_1. \end{aligned} \tag{18}$$

Note that

$$\begin{aligned} \tilde{d}_2 s_2 &\leq \frac{1}{4\varepsilon_2}s_2^2 + \varepsilon_2\tilde{d}_2^2, \\ -s_2\left(\frac{\partial z_2^*}{\partial s_1} + \frac{\partial z_2^*}{\partial \hat{d}_1}\lambda_1\right)\tilde{d}_1 &\leq \frac{1}{4\varepsilon_1}\left(\frac{\partial z_2^*}{\partial s_1} + \frac{\partial z_2^*}{\partial \hat{d}_1}\lambda_1\right)^2 s_2^2 + \varepsilon_1\tilde{d}_1^2 = \hat{c}_2 s_2^2 + \varepsilon_1\tilde{d}_1^2, \end{aligned} \tag{19}$$

by combining (18) and (19) and defining $s_3 = z_3 - z_3^*$, we obtain

$$\dot{V}_2 \leq -Lk_1 s_1^2 - L(\lambda_1 - 2\varepsilon_1)\tilde{d}_1^2 - Lk_2 s_2^2 - L(\lambda_2 - \varepsilon_2)\tilde{d}_2^2 + Ls_2 s_3 + \tilde{d}_2\dot{\tilde{d}}_2 + \tilde{d}_1\dot{\tilde{d}}_1. \quad (20)$$

Following the inductive procedure, assume that at step $i-1$ (for $i \geq 3$), a positive definite and proper Lyapunov function $V_{i-1}(s_1, \ldots, s_{i-1}, \tilde{d}_1, \ldots, \tilde{d}_{i-1})$ has been constructed. The recursive design leads to the following structure for virtual controllers and error variables, the general form of which is summarized by

$$\begin{aligned}
&z_2^* = -\varphi_1 s_1 - \hat{d}_1, && s_2 = z_2 - z_2^*,\\
&z_3^* = -s_1 - (\varphi_2 + \hat{c}_2)\, s_2 - \hat{d}_2 + \frac{\partial z_2^*}{\partial s_1}\left(\hat{d}_1 + z_2\right), && s_3 = z_3 - z_3^*,\\
&\quad\vdots && \quad\vdots\\
&z_{i+1}^* = -s_{i-1} - (\varphi_i + \hat{c}_i)\, s_i - \hat{d}_i + \sum_{j=1}^{i-1}\frac{\partial z_i^*}{\partial z_j}\left(\hat{d}_j + z_{j+1}\right), && s_{i+1} = z_{i+1} - z_{i+1}^*.
\end{aligned} \quad (21)$$

Therefore

`Step i(`$3 \leq i \leq n$`):` A Lyapunov function is defined as presented below

$$V_{i-1} = \sum_{j=1}^{i-1}\frac{1}{2}s_j^2 + \sum_{j=1}^{i-1}\frac{1}{2}\tilde{d}_j^2, \quad (22)$$

taking the derivative gives

$$\dot{V}_{i-1} \leq -L\sum_{j=1}^{i-1}k_j s_j^2 - L\sum_{j=1}^{i-1}(\lambda_j - (i-j)\varepsilon_j)\,\tilde{d}_j^2 + Ls_{i-1}s_i + \sum_{j=1}^{i-1}\tilde{d}_j\dot{\tilde{d}}_j. \quad (23)$$

Set $s_i = z_i - z_i^*$, and define the following Lyapunov function

$$V_i = V_{i-1} + \frac{1}{2}s_i^2 + \frac{1}{2}\tilde{d}_i^2, \quad (24)$$

thus

$$\begin{aligned}
\dot{V}_i \quad \leq \quad & -L\sum_{j=1}^{i-1}k_j s_j^2 - L\sum_{j=1}^{i-1}(\lambda_j - (i-j)\varepsilon_j)\,\tilde{d}_j^2 + Ls_{i-1}s_i\\
& + Ls_i z_{i+1}^* + Ls_i s_{i+1} - L\lambda_i\tilde{d}_i^2\\
& + s_i\left(L\bar{d}_i - \sum_{j=1}^{i-1}\frac{\partial z_i^*}{\partial z_j}\left(Lz_{j+1} + L\bar{d}_j\right) - \sum_{j=1}^{i-1}\frac{\partial z_i^*}{\partial \hat{d}_j}\lambda_j L\tilde{d}_j\right) + \sum_{j=1}^{i}\tilde{d}_j\dot{\tilde{d}}_j.
\end{aligned} \quad (25)$$

Where $s_{i+1} = z_{i+1} - z_{i+1}^*$, The virtual control law is

$$z_{i+1}^* = -s_{i-1} - (\varphi_i + \hat{c}_i)\, s_i - \hat{d}_i + \sum_{j=1}^{i-1}\frac{\partial z_i^*}{\partial z_j}\left(z_{j+1} + \hat{d}_j\right), \quad (26)$$

where $k_i > 0$, $\varepsilon_i > 0$, $\hat{c}_i = \sum_{j=1}^{i-1} \frac{1}{4\varepsilon_j} \left( \frac{\partial z_i^*}{\partial z_j} + \lambda_j \frac{\partial z_i^*}{\partial \hat{d}_j} \right)^2$, and $\varphi_i = k_i + \frac{1}{4\varepsilon_i}$. Incorporating (26) into (25) gives

$$\begin{aligned} \dot{V}_i \leq & -L\sum_{j=1}^{i-1} k_j s_j^2 - L\sum_{j=1}^{i-1} (\lambda_j - (i-j)\varepsilon_j)\, \tilde{d}_j^2 - L\lambda_i \tilde{d}_i^2 - L\left(k_i + \frac{1}{4\varepsilon_i} + \hat{c}_i\right) s_i^2 \\ & + L s_i s_{i+1} + L s_i \tilde{d}_i - L s_i \sum_{j=1}^{i-1} \left( \frac{\partial z_i^*}{\partial z_j} + \lambda_j \frac{\partial z_i^*}{\partial \hat{d}_j} \right) \tilde{d}_j + \sum_{j=1}^{i} \tilde{d}_j \dot{\tilde{d}}_j. \end{aligned} \tag{27}$$

Note that

$$\begin{aligned} s_i \tilde{d}_i &\leq \frac{1}{4\varepsilon_i} s_i^2 + \varepsilon_i \tilde{d}_i^2, \\ -s_i \sum_{j=1}^{i-1} \left( \frac{\partial z_i^*}{\partial z_j} + \lambda_j \frac{\partial z_i^*}{\partial \hat{d}_j} \right) \tilde{d}_j &\leq \sum_{j=1}^{i-1} \frac{1}{4\varepsilon_j} \left( \frac{\partial z_i^*}{\partial z_j} + \lambda_j \frac{\partial z_i^*}{\partial \hat{d}_j} \right)^2 s_i^2 \\ &\quad + \sum_{j=1}^{i-1} \varepsilon_j \tilde{d}_j^2 = \hat{c}_i s_i^2 + \sum_{j=1}^{i-1} \varepsilon_j \tilde{d}_j^2. \end{aligned} \tag{28}$$

Combining (27) and (28), we obtain

$$\dot{V}_i \leq -L\sum_{j=1}^{i} k_j s_j^2 - L\sum_{j=1}^{i} (\lambda_j - (i-j+1)\varepsilon_j)\, \tilde{d}_j^2 + L s_i s_{i+1} + \sum_{j=1}^{i} \tilde{d}_j \dot{\tilde{d}}_j. \tag{29}$$

Specifically, if $i = n$, the practical control signal can be written as

$$\begin{aligned} u &= L^{n+1} z_{n+1}^* \\ &= L^{n+1} \left( -s_{n-1} - \left( k_n + \frac{1}{4\varepsilon_n} + \hat{c}_n \right) s_n - \hat{d}_n + \sum_{j=1}^{n-1} \frac{\partial z_n^*}{\partial z_j} \left( z_{j+1} + \hat{d}_j \right) \right) \end{aligned} \tag{30}$$

where $\hat{c}_n = \sum_{j=1}^{n-1} \frac{1}{4\varepsilon_j} \left( \frac{\partial z_n^*}{\partial z_j} + \lambda_j \frac{\partial z_n^*}{\partial \hat{d}_j} \right)^2$, $\varepsilon_n > 0$, and $k_n > 0$.

**Remark 3.2.** The controller design in Section 3.2 strategically separates the roles of gains: $k_j$ acts as a "stabilizing term", which is retained in the $\dot{V}_n$ analysis in Section 4 to provide negative definiteness and ultimately dominate the upper bound $\kappa$ of the nonlinear term; while $1/4\epsilon_i$ and $\hat{c}_i$ serve as "canceling terms", which are precisely constructed. Their sole purpose is to completely cancel the positive terms generated by the use of Young's inequality in derivations. This design ensures that only the desired $-Lk_j s_j^2$ stabilizing term is retained in the final $\dot{V}_n$ inequality, thereby greatly simplifying the stability proof.

## 4. STABILITY ANALYSIS

### 4.1. Stability analysis for the nominal system

The closed-loop system is rewritten as

$$\begin{aligned}
\dot{s}_1 &= Ls_2 - L\varphi_1 s_1 + L\tilde{d}_1, \\
\dot{s}_2 &= Ls_3 - Ls_1 - L\left(\varphi_2 + \hat{c}_2\right) s_2 + L\tilde{d}_2 - \frac{\partial z_2^*}{\partial \hat{d}_1}\lambda_1 L\tilde{d}_1 - \frac{\partial z_2^*}{\partial s_1} L\tilde{d}_1, \\
&\vdots \\
\dot{s}_n &= -Ls_{n-1} - L\left(\varphi_n + \hat{c}_n\right) s_n + L\tilde{d}_n - L\sum_{j=1}^{n-1}\frac{\partial z_n^*}{\partial \hat{d}_j}\lambda_j \tilde{d}_j - L\sum_{j=1}^{n-1}\frac{\partial z_n^*}{\partial z_j}\tilde{d}_j, \qquad (31) \\
\dot{\tilde{d}}_i &= \dot{\tilde{d}}_i - \lambda_i L\tilde{d}_i, \qquad (32) \\
y &= x_1 = Ls_1.
\end{aligned}$$

**Theorem 4.1.** The composite system of (31) and (32) is globally ISS, provided that the disturbances acting on system (1) satisfy the boundedness conditions stated in Assumption 2.

P r o o f . Construct the Lyapunov function as

$$V_n = \sum_{i=1}^{n}\frac{1}{2}s_i^2 + \sum_{i=1}^{n}\frac{1}{2}\tilde{d}_i^2. \qquad (33)$$

The differentiation of $V_n$ in the closed-loop system gives

$$\dot{V}_n \le -L\sum_{j=1}^{n} k_j s_j^2 - L\sum_{j=1}^{n}\left(\lambda_j - (n-j+1)\varepsilon_j\right)\tilde{d}_j^2 + \sum_{j=1}^{n}\tilde{d}_j\dot{\tilde{d}}_j. \qquad (34)$$

By choosing $\lambda_j = a_{0j} + (n-j+1)\varepsilon_j (a_{0j} > 0)$, then (34) becomes

$$\begin{aligned}
\dot{V}_n &\le -L\sum_{j=1}^{n} k_j s_j^2 - L\sum_{j=1}^{n} a_{0j}\tilde{d}_j^2 + \sum_{j=1}^{n}\tilde{d}_j\dot{\tilde{d}}_j \\
&\le -L\sum_{j=1}^{n} k_j s_j^2 - a_0 L\|\tilde{d}\|^2 + \|\tilde{d}\|\|\dot{\tilde{d}}\|, \qquad (35)
\end{aligned}$$

where $\tilde{d} = [\tilde{d}_1, \ldots, \tilde{d}_n]^T, \dot{\tilde{d}} = [\dot{\tilde{d}}_1, \ldots, \dot{\tilde{d}}_n]^T, a_0 = \min\{a_{01}, \ldots, a_{0n}\}$, and $k_{\min} = \min\{k_1, \ldots, k_n\}$. Furthermore, inequality (35) becomes

$$\dot{V}_n \le -Lk_{\min}\sum_{j=1}^{n} s_j^2 - (1-\theta)a_0 L\|\tilde{d}\|^2 - \theta a_0 L\|\tilde{d}\|^2 + \|\tilde{d}\|\|\dot{\tilde{d}}\|, \qquad (36)$$

in which $0 < \theta < 1$. Considering the case where $\|\tilde{d}\| \ge \|\dot{\tilde{d}}\|/a_0\theta L$, the above inequality simplifies to $\dot{V}_n \le -Lk_{\min}\sum_{j=1}^{n} s_j^2 - (1-\theta)a_0 L\|\tilde{d}\|^2$. This directly satisfies the conditions of Lemma 2.5, proving the global ISS of the interconnected systems (31) and (32). □

**Remark 4.2.** The problem of global stabilization for a class of disturbed nonlinear systems (1) with known nonlinear functions has been extensively reported in the literature, such as [24, 30]. The core challenge of this paper lies in handling unknown nonlinear functions $f_i$, where it is only know that they satisfy the linear growth condition in Assumption 2.1. Theorem 4.1 provides the conclusion that the nominal system (31) – (32) is globally ISS, which does not account for the unknown nonlinear terms $f_i$. Next, it will be shown how, by introducing the high gain $L$, the total disturbance term $T_f$ generated by the unknown nonlinear terms $f_i$ (in equation 39) can be suppressed by $L$. This is the core mechanism ensuring that the complete system (37) with unknown nonlinearities ultimately achieves global stability.

**Theorem 4.3.** Under Assumption 2.2 and provided that the disturbance derivatives asymptotically tend to zero, i. e., $\lim_{t\to\infty} \dot{d}_i(t) = 0$, the presented control scheme ensures that both the output $y$ and the disturbance estimation errors $\tilde{d}_i$ of the composite system (31) – (32) asymptotically converge to zero.

P r o o f. Globally ISS of system (31) – (32) has been proven in Theorem 4.1, considering $\dot{\bar{d}}$ as the external input. Recalling the coordinate transformation $\bar{d}_i = d_i/L^{i+1}$ from (5) – (6), and the premise $\lim_{t\to\infty} \|\dot{d}(t)\| = 0$, the asymptotic vanishing of the input $\dot{\bar{d}}(t)$ is assured for constant $L > 1$. In light of Lemma 2.6, a vanishing input to an ISS system forces the asymptotic convergence of its states, i. e., $\lim_{t\to\infty} s_i(t) = 0$ and $\lim_{t\to\infty} \tilde{d}_i(t) = 0$. This result, combined with the output equation $y = x_1 = Ls_1$, completes the proof that $y(t) \to 0$. □

### 4.2. Stability analysis for the complete system

Now, we consider the following augmented system:

$$\begin{cases} \dot{z}_i &= Lz_{i+1} + L\bar{d}_i + \frac{f_i}{L^i}, \\ \dot{\tilde{d}}_i &= \dot{\bar{d}}_i - \lambda_i L\tilde{d}_i - \lambda_i \frac{f_i}{L^i}, \\ \dot{\hat{d}}_i &= \lambda_i L\tilde{d}_i + \lambda_i \frac{f_i}{L^i}. \end{cases} \tag{37}$$

from which Theorem 4.4 can be derived.

**Theorem 4.4.** Under Assumptions 2.1 and 2.2, if the composite controller proposed in Section 3 is applied with a sufficiently large gain $L$, then the closed-loop system (37) is globally ISS.

P r o o f. Considering the same Lyapunov function $V_n$ defined in (33), its derivative along (37) follows from (35) as

$$\begin{aligned} \dot{V}_n \leq\ & -L\sum_{j=1}^{n} k_j s_j^2 - L\sum_{j=1}^{n} a_{0j}\tilde{d}_j^2 + \sum_{j=1}^{n} \tilde{d}_j\dot{\tilde{d}}_j + \sum_{j=1}^{n} \frac{s_j f_j}{L^j} \\ & - \sum_{j=1}^{n} \frac{\lambda_j f_j \tilde{d}_j}{L^j} - \sum_{i=2}^{n} s_i \sum_{j=1}^{i-1} \left( \frac{\partial z_i^*}{\partial z_j} + \frac{\partial z_i^*}{\partial \hat{d}_j}\lambda_j \right) \frac{f_j}{L^j}. \end{aligned} \tag{38}$$

Let the expression involving the nonlinear functions $f_i$ in (38) be denoted as

$$T_f = \sum_{j=1}^{n} \frac{s_j f_j}{L^j} - \sum_{j=1}^{n} \frac{\lambda_j f_j \tilde{d}_j}{L^j} - \sum_{i=2}^{n} s_i \sum_{j=1}^{i-1} \left( \frac{\partial z_i^*}{\partial z_j} + \frac{\partial z_i^*}{\partial \hat{d}_j} \lambda_j \right) \frac{f_j}{L^j}, \tag{39}$$

where $s_j$ and $\tilde{d}_j$ denote the state variables of the Lyapunov function $V_n$, $L > 1$ represents the control gain, $\lambda_j$ signifies the observer gain, and $z_n^*$ denotes the virtual control input.

It follows from Assumption 2.1 and the relation $z_k = x_k/L^k$ that

$$|f_j| \leq \gamma_j \sum_{k=1}^{j} L^k |z_k|. \tag{40}$$

The variable $z_k$ is related to $s_k$ as follows: $s_1 = z_1$, and for $k \geq 2$, $s_k = z_k - z_k^*$. The virtual control input $z_k^*$ is a function of $s_1, \ldots, s_{k-1}$ and $\hat{d}_1, \ldots, \hat{d}_{k-1}$.Since $\hat{d}_j = \bar{d}_j - \tilde{d}_j$ and $\bar{d}_j$ is bounded, the bound of $|z_k^*|$ can be derived. Specifically, one can find a constant $c > 0$ (determined by system gains and design parameters) such that

$$|z_k| \leq |s_k| + |z_k^*| \leq |s_k| + c \sum_{m=1}^{k-1} \big( |s_m| + |\tilde{d}_m| \big). \tag{41}$$

Substituting the bound of $|f_j|$

$$|f_j| \leq \gamma_j \sum_{k=1}^{j} L^k \Big( |s_k| + c \sum_{m=1}^{k-1} \big( |s_m| + |\tilde{d}_m| \big) \Big). \tag{42}$$

In $T_f$, each term contains a factor of $\dfrac{1}{L^j}$. Therefore, consider $\left| \dfrac{f_j}{L^j} \right|$

$$\left| \frac{f_j}{L^j} \right| \leq \frac{\gamma_j}{L^j} \sum_{k=1}^{j} L^k |z_k| \leq \gamma_j \sum_{k=1}^{j} L^{k-j} \Big( |s_k| + c \sum_{m=1}^{k-1} \big( |s_m| + |\tilde{d}_m| \big) \Big). \tag{43}$$

Since $L > 1$ and $k \leq j$, it can be deduced that $L^{k-j} \leq 1$. Further simplification gives

$$\left| \frac{f_j}{L^j} \right| \leq \gamma_j \sum_{k=1}^{j} |s_k| + \gamma_j c \sum_{k=1}^{j} \sum_{m=1}^{k-1} |s_m| + \gamma_j c \sum_{k=1}^{j} \sum_{m=1}^{k-1} |\tilde{d}_m|. \tag{44}$$

Where

$$\begin{aligned} \sum_{k=1}^{j} \sum_{m=1}^{k-1} |s_m| &= \sum_{m=1}^{j-1} |s_m|(j-m) \leq j \sum_{m=1}^{j-1} |s_m|, \\ \sum_{k=1}^{j} \sum_{m=1}^{k-1} |\tilde{d}_m| &= \sum_{m=1}^{j-1} |\tilde{d}_m|(j-m) \leq j \sum_{m=1}^{j-1} |\tilde{d}_m|. \end{aligned} \tag{45}$$

Thus, combining Formulas (44) and (45) yields

$$\left|\frac{f_j}{L^j}\right| \leq \gamma_j(1+cj)\sum_{k=1}^{j}|s_k| + \gamma_j cj\sum_{m=1}^{j-1}|\tilde{d}_m|. \tag{46}$$

Now, each term in $T_f$ can be bounded individually.

$$\begin{aligned}
&\left|\frac{s_j f_j}{L^j}\right| \leq |s_j|\left|\frac{f_j}{L^j}\right| \leq |s_j|\left(\gamma_j(1+cj)\sum_{k=1}^{j}|s_k| + \gamma_j cj\sum_{m=1}^{j-1}|\tilde{d}_m|\right),\\
&\left|\frac{\lambda_j f_j \tilde{d}_j}{L^j}\right| \leq \lambda_j|\tilde{d}_j|\left|\frac{f_j}{L^j}\right| \leq \lambda_j|\tilde{d}_j|\left(\gamma_j(1+cj)\sum_{k=1}^{j}|s_k| + \gamma_j cj\sum_{m=1}^{j-1}|\tilde{d}_m|\right),\\
&\left|s_i\sum_{j=1}^{i-1}\left(\frac{\partial z_n^*}{\partial z_j} + \frac{\partial z_n^*}{\partial \hat{d}_j}\lambda_j\right)\frac{f_j}{L^j}\right| \leq \sum_{j=1}^{i-1}|s_i||c_j|\left|\frac{f_j}{L^j}\right|.
\end{aligned} \tag{47}$$

Where $c_j = \frac{\partial z_n^*}{\partial z_j} + \frac{\partial z_n^*}{\partial \hat{d}_j}\lambda_j$, and $|c_j|$ is bounded.

Using Young's inequality ($ab \leq \frac{a^2}{2\epsilon} + \frac{\epsilon b^2}{2}$) to handle these product terms. For example:

$$|s_j|\sum_{k=1}^{j}|s_k| \leq \frac{1}{2\epsilon}s_j^2 + \frac{\epsilon}{2}\left(\sum_{k=1}^{j}|s_k|\right)^2 \leq \frac{1}{2\epsilon}s_j^2 + \frac{\epsilon}{2}\cdot j\sum_{k=1}^{j}s_k^2. \tag{48}$$

Similarly handle the other terms. Eventually, $|T_f|$ can be bounded as

$$|T_f| \leq \kappa\sum_{j=1}^{n}(s_j^2 + \tilde{d}_j^2). \tag{49}$$

The positive constant $\kappa > 0$ denotes a parameter that depends on $\gamma_j, c, j, \lambda_j$ and the system order $n$, etc. Substituting into formula (38), the Lyapunov derivative becomes

$$\begin{aligned}
\dot{V}_n &\leq -L\sum_{j=1}^{n}k_j s_j^2 - L\sum_{j=1}^{n}a_{0j}\tilde{d}_j^2 + \sum_{j=1}^{n}\tilde{d}_j\dot{\tilde{d}}_j + T_f\\
&\leq -L\sum_{j=1}^{n}k_j s_j^2 - L\sum_{j=1}^{n}a_{0j}\tilde{d}_j^2 + \sum_{j=1}^{n}\tilde{d}_j\dot{\tilde{d}}_j + \kappa\sum_{j=1}^{n}(s_j^2 + \tilde{d}_j^2).
\end{aligned} \tag{50}$$

It follows from formulas (36) and (50) that

$$\dot{V}_n \leq -(Lk_{\min} - \kappa)\sum_{j=1}^{n}s_j^2 - (1-\theta)a_0 L\|\tilde{d}\|^2 - (\theta a_0 L - \kappa)\|\tilde{d}\|^2 + \|\tilde{d}\|\|\dot{\tilde{d}}\|. \tag{51}$$

When $L$ is sufficiently large, it follows that

$$Lk_{\min} - \kappa > 0, \quad a_0\theta L - \kappa > 0, \quad \|\tilde{d}\| \geq \frac{\|\dot{\tilde{d}}\|}{a_0\theta L - \kappa}. \tag{52}$$

The preceding analysis satisfies the conditions of Lemma 2.5, and thus the closed-loop system (37) can be declared globally ISS. □

**Remark 4.5.** The selection of the scaling gain $L$ involves a fundamental trade-off between robustness and practical implementation. Theoretically, $L$ must be sufficiently large to satisfy $Lk_{\min} - \kappa > 0$, so that the high-gain term dominates the unknown nonlinearities and mismatched disturbances. In practice, however, an excessively large $L$ may cause two adverse effects: (i) the peaking phenomenon, where initial estimation errors amplified by high powers of $L$ lead to transient overshoots and potential actuator saturation; and (ii) increased sensitivity to high-frequency measurement noise due to the elevated system bandwidth, which degrades steady-state tracking performance. Therefore, a practical alternative is to adopt a piecewise constant gain profile: keeping the scaling gain $L$ at a moderate value during the initial transient phase can mitigate the peaking phenomenon and noise sensitivity to a certain extent, followed by a gradual increase to the theoretically required high-gain value, thereby achieving strong disturbance rejection without sacrificing transient performance. Since Theorem 4.4 guarantees ISS for any constant gain meeting the stability bound, the closed-loop system retains its stability under such a piecewise constant schedule, provided the gain is eventually chosen sufficiently large. As designed in Example 1.

**Remark 4.6.** The control scheme put forward herein constitutes a composite control design. It recursively integrates a nonlinear disturbance observer for handling mismatched and non-vanishing disturbances, as well as a high-gain scaling technique for dealing with unknown nonlinear functions $f_i$. This is fundamentally different in design philosophy from traditional model-based nonlinear control methods. Traditional methods typically attempt to cancel the influence of nonlinear functions $f_i$ through accurate model information. In contrast, the proposed method only requires them to satisfy the linear growth condition, and this design framework endows the controller with stronger robustness against model parameter uncertainties.

**Remark 4.7.** It is worth emphasizing that the composite control framework proposed in this paper can be extended to more general classes of systems. For interconnected systems, provided that each subsystem satisfies the linear growth condition and the interconnection terms also obey the linear growth property, the coupling effects among subsystems can be effectively suppressed by appropriately increasing the scaling gain $L$. In this way, the stability of the entire network can be guaranteed without strictly relying on the small-gain condition. In addition, by virtue of high-gain scaling to dominate non-triangular dynamics, the developed framework is applicable to non-strict-feedback systems. Furthermore, through matrix-based scaling design and vector-valued disturbance observers, the proposed method can be generalized to multi-input multi-output nonlinear systems, realizing robust disturbance compensation for each control channel.

## 5. SIMULATION EXAMPLES

### 5.1. Example 1: A second-order strict-feedback system

Consider the following second-order strict-feedback system, whose governing equations are given by

$$\begin{aligned} \dot{x}_1 &= x_2 + f_1(x_1) + d_1(t), \\ \dot{x}_2 &= u + f_2(x_1, x_2) + d_2(t), \\ y &= x_1. \end{aligned} \tag{53}$$

Specifically, $f_1(x_1) = 0.5\sin(x_1)$ and $f_2(x_1, x_2) = 0.5\sin(x_1) + 0.5\tanh(x_2)$ both satisfy Assumption 2.1 in this paper. For comparison, integral backstepping controller [8], the composite controller [24], the high-gain backstepping controller and the neural network-based composite anti-disturbance controller [23] are also applied to this example (see Appendix for details).

For simulation purposes, the following specific forms of $f_i$ are used. It is crucial to note that this information is only used to simulate the controlled plant, and the controller proposed herein does not use this information at all in design and implementation. This fully verifies the robustness of the proposed method.

Controller parameter design: For the method in this paper, the scaling gain $L$ is designed as a piecewise variable parameter: $L = 2$ for $t < 30$ s, then linearly increases to 10 during $t \in [30, 35]$ s, and remains at 10 thereafter. The other control gains are chosen as $k_1 = 0.5$, $k_2 = 1$, $\lambda_1 = \lambda_2 = 5$, $\epsilon_1 = \epsilon_2 = 1$; for the high-gain backstepping controller, $l_1 = 15$, $l_2 = 20$; for the integral backstepping controller, $\beta_0 = \beta_1 = 2$, $\beta_2 = 3$; for the composite controller combining backstepping control and disturbance observer, $k_1 = k_2 = 2$, $\lambda_1 = \lambda_2 = 15$, $\epsilon_1 = \epsilon_2 = 10$. For the neural network-based composite anti-disturbance controller, $k_1 = 5$, $k_2 = 10$, $L_1 = \begin{bmatrix} -0.6813 & -0.46884 \end{bmatrix}^T$, $L_2 = \begin{bmatrix} -0.07666 & 0.08002 \end{bmatrix}^T$, $\Gamma_2 = 20$, and $N = 90$ ($N$ is the dimension of $\theta_2$). The centers of radial basis functions (RBFs) evenly cover the compact set $[-1, 1] \times [-11, 11]$, and the widths of RBFs are selected to be $\sigma = 2.4$.

The initial values are chosen as $x(0) = [1, -1]^T$. The system is then under the action of an external disturbance defined as

$$d_1(t) = \begin{cases} 0, & t \in [0, 15) \cup [25, 35) \\ 2, & t \in [15, 25) \\ 0.5\sin(t), & t \in [35, +\infty) \end{cases}, \; d_2(t) = \begin{cases} 0, & t \in [0, 15) \cup [25, 35) \\ 1, & t \in [15, 25) \\ 0.6\cos(t), & t \in [35, +\infty) \end{cases}.$$

The simulation results are presented in Figures 1, 2, and Table 1. As can be seen from Figure 2, the proposed composite anti-disturbance control method achieves superior disturbance rejection performance. In contrast, the traditional high-gain backstepping and integral backstepping methods exhibit issues of excessive control effort or significant steady-state error, respectively, when dealing with unmatched disturbances and mismatched nonlinearities. It is noteworthy that although the model-based composite controller from [24] can also achieve satisfactory dynamic response, its design process heavily relies on precise model information of the nonlinear functions, thus limiting its robustness. In comparison, the method presented in this paper achieves comparable or even better control performance without requiring any prior knowledge of the nonlinear models.

Furthermore, as can be seen from Figure 2, compared with the neural network-based intelligent control strategy, the proposed method directly suppresses unknown nonlinearities through a simple high-gain linear structure, achieving comparable or even slightly better anti-disturbance performance under both constant and periodic disturbances.

More importantly, this method completely eliminates the inherent complex weight updates and matrix operations involved in the online learning process. As shown in Table 1, under identical simulation conditions, the proposed method significantly reduces the CPU running time and greatly lowers the memory footprint, demonstrating a clear computational efficiency advantage that makes it more suitable for real-time engineering implementation.

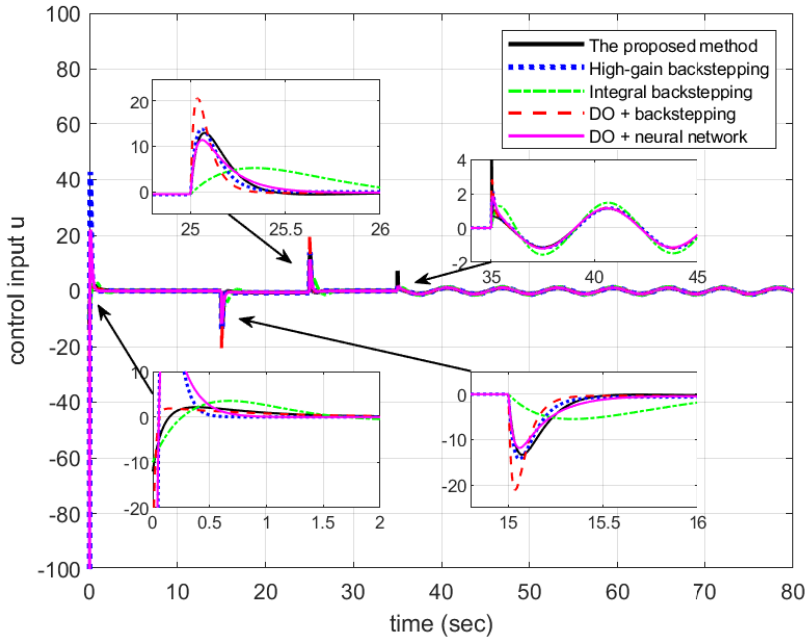



**Fig. 1.** Input trajectories for numerical simulation (53) under the proposed (black solid), disturbance observer-backstepping (red dashed), high-gain backstepping (blue dotted), neural network-based composite anti-disturbance control (magenta solid) and integral backstepping (green dash-dotted) methods.

| Controller Type | CPU Execution Time (s) | Memory Usage(KB) |
|---|---|---|
| The proposed method | 0.0819 | 407.53 |
| DO + neural network | 0.3617 | 5040.75 |

**Tab. 1.** Quantitative Performance Comparison.

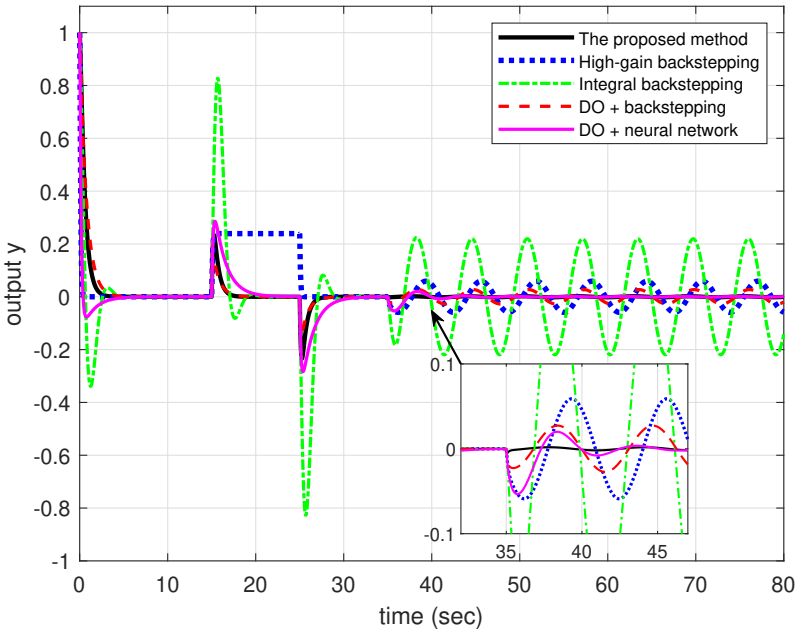



**Fig. 2.** Output trajectories for numerical simulation (53) under the proposed (black solid), disturbance observer-backstepping (red dashed), high-gain backstepping (blue dotted), neural network-based composite anti-disturbance control (magenta solid) and integral backstepping (green dash-dotted) methods.

### 5.2. Example 2: Application to a single-link robotic arm

We consider the model of a single-link robotic arm system given in [26]:

$$\begin{aligned}
\dot{q}_1 &= q_2, \\
\dot{q}_2 &= \frac{K}{J_2 N} q_3 - \frac{F_2(t)}{J_2} q_2 - \frac{K}{J_2} q_2 - \frac{mgd}{J_2} \cos q_1, \\
\dot{q}_3 &= q_4, \\
\dot{q}_4 &= \frac{1}{J_1} u + \frac{K}{J_1 N} q_1 - \frac{K}{J_2 N} q_3 - \frac{F_1(t)}{J_1} q_4, \\
y &= q_1.
\end{aligned} \tag{54}$$

Here, $J_1$, $J_2$, $K$, $N$, $m$, $g$, and $d$ are known constants of the system. The viscous friction coefficients $F_1(t)$ and $F_2(t)$ vary around their known nominal values $F_{10}$ and $F_{20}$, respectively.

And through the following coordinate transformation

$$x_1 = q_1,\ x_2 = q_2,\ x_3 = \frac{K}{J_2 N} q_3 - \frac{mgd}{J_2},$$
$$x_4 = \frac{K}{J_2 N} q_4,\ u = \frac{K}{J_2 N}\left(\frac{u}{J_1} - \frac{mgd}{J_2}\right).$$

The system can be transformed into

$$\begin{aligned}
\dot{x}_1 &= x_2, \\
\dot{x}_2 &= x_3 - \frac{F_2}{J_2}\left(x_2 + \frac{K}{F_{20}} x_1 + \frac{mgd}{F_{20}}(\cos x_1 - 1)\right) + d_1(t), \\
\dot{x}_3 &= x_4, \\
\dot{x}_4 &= u - \frac{F_1}{J_1}\left(x_4 - \frac{K^2}{J_2 N^2 F_{10}} x_1 + \frac{J_1 K}{J_2 N F_{10}} x_3\right) + d_2(t), \\
y &= x_1.
\end{aligned} \tag{55}$$

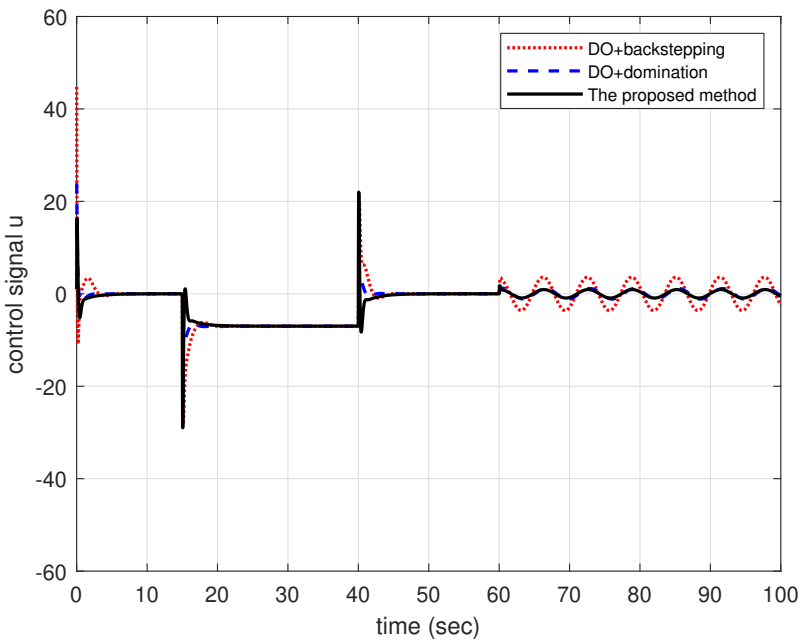



**Fig. 3.** Input trajectories of application simulation (54) under the three controllers. The responses of the proposed method, disturbance observer-backstepping method, and homogeneous dominance-based disturbance observer control are depicted as black solid, red dotted and blue dashed lines, respectively.

In particular, the nonlinearities $f_2 = -\frac{F_2}{J_2}\left(x_2 + \frac{K}{F_{20}}x_1 + \frac{mgd}{F_{20}}(\cos x_1 - 1)\right)$ and $f_4 = -\frac{F_1}{J_1}\left(x_4 - \frac{K^2}{J_2 N^2 F_{10}}x_1 + \frac{J_1 K}{J_2 N F_{10}}x_3\right)$ associated with the system both meet the criteria of Assumption 2.1.

In this study, the external disturbances are considered to be

$$d_1(t) = \begin{cases} 0, & t \in [0,15) \cup [40,60) \\ 2, & t \in [15,40) \\ 0.2\sin(t), & t \in [60,+\infty) \end{cases}, \; d_2(t) = \begin{cases} 0, & t \in [0,15) \cup [40,60) \\ 1, & t \in [15,40) \\ 0.8\cos(t), & t \in [60,+\infty) \end{cases}.$$

During the simulation process, the parameters are configured to: $J_1 = 9$ kg $\cdot$ m$^2$, $J_2 = 2$ kg $\cdot$ m$^2$, $N = 5/3$, $K = 10$ N $\cdot$ m/rad, $mgd = 8$ N $\cdot$ m (where $m$ is in kg, $g$ in m/s$^2$, and $d$ in m), $F_{10} = 18$ N $\cdot$ m $\cdot$ s/rad, $F_{20} = 10$ N $\cdot$ m $\cdot$ s/rad; the initial values are selected as $[x_{10}, x_{20}, x_{30}, x_{40}] = [0.7, -0.5, -1, -1]$.

Controller parameter design: For the method in this work, $L = 2.2$, $k_1 = k_2 = k_3 = 0.2$, $k_4 = 0.5$, $\lambda_1 = \lambda_2 = 0.5$, For the method in reference [24], $k_1 = 4$, $k_2 = k_3 = k_4 = 3$, $\lambda_1 = \lambda_2 = 4$, $\epsilon = 500$, For the method in reference [30], $k_1 = k_2 = k_3 = 2$, $k_4 = 1$, $\lambda_1 = \lambda_2 = 7$.

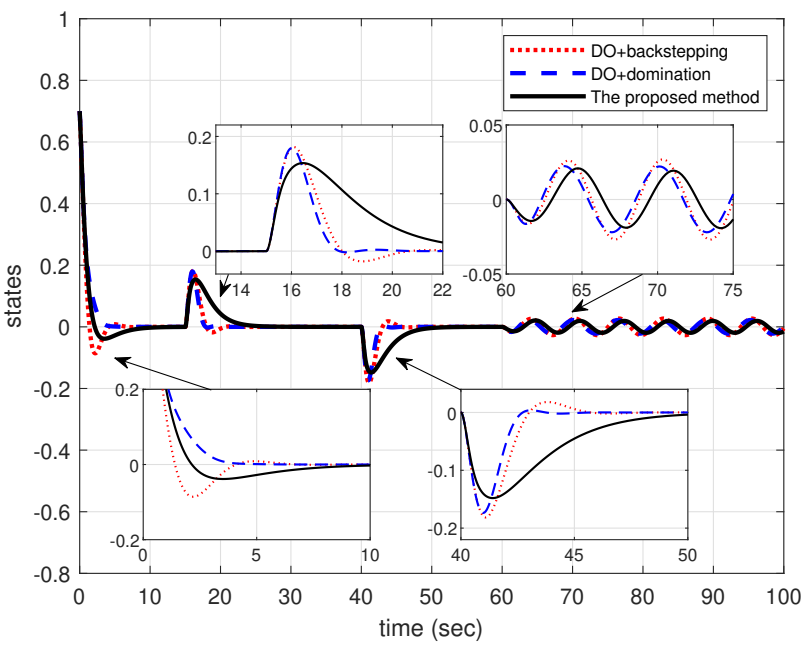



**Fig. 4.** State trajectories of application simulation (54) under the three controllers. The responses of the proposed method, disturbance observer-backstepping method, and homogeneous dominance-based disturbance observer control are depicted as black solid, red dotted and blue dashed lines, respectively.

As shown in Figures 4 and 5 that the proposed method has the minimum initial energy requirement, but its convergence speed is slightly slower than that of the other two comparative methods. This behavior reflects an expected theoretical trade-off inherent in designs that do not rely on accurate nonlinear model information. However, this trade-off brings significant robustness advantages: under the disturbances at $t = 15\,\mathrm{s}$, $40\,\mathrm{s}$, and $60\,\mathrm{s}$, the proposed method exhibits the smallest state fluctuations and the strongest disturbance rejection capability, thus demonstrating stronger adaptability in the face of model uncertainties.

## 6. CONCLUSION

This paper has addressed the global output regulation problem for strict-feedback systems with unknown nonlinearities and mismatched persistent disturbances. The solution synthesizes a high-gain observer into a composite robust control framework. Key to this approach is a high-gain coordinate transformation that suppresses the influence of nonlinear terms under only a linear growth condition, coupled with a recursively designed nonlinear disturbance observer that delivers accurate estimation and feedforward compensation of the mismatched disturbances. The input-to-state stability of the resulting closed-loop system is rigorously proven via Lyapunov analysis. Numerical simulations corroborate the superiority and effectiveness of the proposed strategy in handling system uncertainties.

## APPENDIX A: CONTROLLER IN THE NUMERICAL SIMULATION

For the convenience of readers, this section provides the details of the high-gain backstepping controller used in the numerical simulations of (53), the integral backstepping method from [8], and the composite anti-disturbance control method based on neural networks from [23]. Below is the description of the high-gain backstepping controller

$$u = -z_1 - l_2 z_2 - f_2(x_1, x_2) + \frac{\partial x_2^*}{\partial x_1}(x_2 + f_1(x_1)), \tag{56}$$

where

$$z_1 = x_1, z_2 = x_2 - x_2^*, \quad x_2^* = -l_1 x_1 - f_1(x_1).$$

Here, $l_1$ and $l_2$ represent positive constant gains.

The expression of the integral backstepping controller is presented as

$$u = -z_1 - f_2(x_1, x_2) + \frac{\partial x_2^*}{\partial x_0} x_1 + \frac{\partial x_2^*}{\partial x_1}(x_2 + f_1(x_1)) - \beta_2 z_2. \tag{57}$$

with

$$\begin{aligned} z_2 = x_2 - x_2^*, \quad x_0 = \int_0^t x_1 \,\mathrm{d}s, \\ x_2^* = -x_0 - f_1(x_1) - \beta_0 x_1 - \beta_1 \hat{z}_1, \\ \hat{z}_1 = x_1 - \bar{x}_1^*, \quad \bar{x}_1^* = -\beta_0 x_0. \end{aligned}$$

In this context, $\beta_0$, $\beta_1$ and $\beta_2$ are positive constants.

The neural network-based composite anti-disturbance controller is given by

$$\begin{aligned}
u &= -z_1 - k_2 z_2 - \frac{1}{\eta_2} z_2 - \frac{1}{\eta_2}\left(\frac{\partial \alpha_1}{\partial z_1}\right)^2 z_2 \\
&\quad - \frac{1 + \left\|L_1^T V_1^T\right\|^2}{2\eta_2}\left(\frac{\partial \alpha_1}{\partial \hat{d}_1}\right)^2 z_2 - \hat{d}_2 - \theta_2^T \xi_2 \\
&\quad + \frac{\partial \alpha_1}{\partial z_1}(\hat{d}_1 + x_2) + \frac{\partial \alpha_1}{\partial \hat{d}_1} V_1\big((G_1 + L_1 V_1)\hat{\omega}_1 - L_1 \hat{d}_1\big) \\
&\quad + \frac{\partial \alpha_1}{\partial y_r}\dot{y}_r + \frac{\partial \alpha_1}{\partial \dot{y}_r}\ddot{y}_r. \qquad (58) \\
\dot{v}_1 &= (G_1 + L_1 V_1)(v_1 - L_1 x_1) + L_1 x_2, \\
\dot{v}_2 &= (G_2 + L_2 V_2)(v_2 - L_2 x_2) + L_2\big(u + \theta_2^T \xi_2\big), \\
\hat{\omega}_i &= v_i - L_i x_i, \quad \hat{d}_i = V_i \hat{\omega}_i, \quad i = 1, 2 \\
\alpha_1 &= -k_1 z_1 - \hat{d}_1 + \dot{y}_r, \\
z_1 &= x_1 - y_r, \quad z_2 = x_2 - \alpha_1,
\end{aligned}$$

where $k_1$ and $k_2$ are positive constants.

## APPENDIX B: CONTROLLER IN THE APPLICATION SIMULATION

For comparative simulation studies, the nonlinear controllers presented in [24] and [30] for the single-link robotic manipulator system (54) are utilized, serving as benchmarks against the proposed approach.

The controller introduced in Reference [24] is detailed below

$$\begin{aligned}
&\hat{d}_1 = \lambda_1(x_2 - p_1), \quad \hat{d}_2 = \lambda_2(x_4 - p_2), \\
&\hat{p}_1 = x_3 + f_2 + \hat{d}_1, \quad \hat{p}_2 = v + f_4 + \hat{d}_2, \\
&z_1 = x_1, \quad z_i = x_i - x_i^*, \quad i \in \mathbb{N}_2, 4 \\
&\hat{c}_2 = \frac{1}{4\epsilon}\left(\frac{\partial x_3^*}{\partial x_1}\right)^2, \\
&\hat{c}_3 = \frac{1}{4\epsilon}\left(\frac{\partial x_4^*}{\partial x_1}\right)^2 + \frac{1}{4\epsilon}\left(\frac{\partial x_4^*}{\partial d_1} + \lambda_1 \frac{\partial x_3^*}{\partial x_1}\right)^2, \\
&\hat{c}_4 = \frac{1}{4\epsilon}\left(\frac{\partial x_4^*}{\partial x_1}\right)^2 + \frac{1}{4\epsilon}\left(\frac{\partial x_4^*}{\partial x_2} + \lambda_1 \frac{\partial x_4^*}{\partial d_1}\right)^2 + \frac{1}{4\epsilon}\left(\frac{\partial x_4^*}{\partial x_3}\right)^2, \\
&x_2^* = -\left(k_1 + \frac{1}{4\epsilon}\right) z_1, \\
&x_3^* = -z_1 - \left(k_2 + \frac{1}{4\epsilon} + \hat{c}_2\right) z_2 - \hat{d}_1 - f_2 - \frac{\partial x_2^*}{\partial x_1} x_2, \\
&x_4^* = -z_2 - \left(k_3 + \frac{1}{4\epsilon} + \hat{c}_3\right) z_3 + \frac{\partial x_3^*}{\partial x_1} x_2 + \frac{\partial x_3^*}{\partial x_2}(x_3 + f_2 + \hat{d}_1),
\end{aligned}$$

$$u = -z_3 - \left(k_4 + \frac{1}{4\epsilon} + \hat{c}_4\right) z_4 - f_4 - \hat{d}_2 + \frac{\partial x_4^*}{\partial x_1} x_2 + \frac{\partial x_4^*}{\partial x_2}(x_3 + f_2 + \hat{d}_1) + \frac{\partial x_4^*}{\partial x_3} x_4, \quad (59)$$

where $f_2 = -\frac{F_{\Omega 0}}{J_2} x_2 - \frac{K}{J_2} x_1 - \frac{mgd}{J_2}(\cos x_1 - 1)$, $f_4 = \frac{K^2}{J_1 J_2 N^2} x_1 - \frac{K}{J_2 N} x_3 - \frac{F_{\Omega 0}}{J_1} x_4$, and $\epsilon > 0$ is a design parameter.

The controller introduced in Reference [30] is detailed below

$$\begin{aligned} &\hat{d}_1 = \lambda_1(x_2 - p_1), \quad \hat{d}_2 = \lambda_2(x_4 - p_2), \\ &\dot{p}_1 = x_3 + f_2 + \hat{d}_1, \quad \dot{p}_2 = v + f_4 + \hat{d}_2, \\ &u = -k_4 \left(x_4 + k_3 \left(x_3 + k_2 \left(x_2 + k_1 x_1\right) + \hat{f}_2 + \hat{d}_1\right)\right) - \hat{f}_4 - \hat{d}_2, \end{aligned} \quad (60)$$

where $\hat{f}_2 = 0$ and $\hat{f}_4 = \frac{K \hat{d}_1}{J_2 N}$.

## ACKNOWLEDGEMENT

This work was supported in part by the Zhejiang Provincial Natural Science Foundation of China (LY23F030005, LY24F030011, LQ24F030011), and the National Natural Science Foundation of China (62373131, 62303147).

(Received December 26, 2025)

## REFERENCES

[1] D. Astolfi and G. Casadei: Stabilization of nonlinear systems in presence of filtered output via extended high-gain observers. Automatica *110* (2019), 108594. DOI: 10.1016/j.automatica.2019.108594

[2] Ö. Bingöl and H. M. Güzey: Design of a neuro-sliding mode controller for interconnected quadrotor UAVs carrying a suspended payload. Kybernetika *59* (2023), 670–699. DOI: 10.14736/kyb-2023-5-0670

[3] M. Chen and S. S. Ge: Adaptive neural output feedback control of uncertain nonlinear systems with unknown hysteresis using disturbance observer. IEEE Trans. Ind. Electron. *62* (2015), 7706–7716. DOI: 10.1109/TIE.2015.2455053

[4] J. Davila: Exact tracking using backstepping control design and high-order sliding modes. IEEE Trans. Automat. Control *58* (2013), 2077–2081. DOI:10.14736/kyb-2025-1-0032

[5] W. He, J. Guo, and Z. Xiang: Disturbance-observer-based sampled-data adaptive output feedback control for a class of uncertain nonlinear systems. Int. J. Syst. Sci. *50* (2019), 1771–1783. DOI: 10.1080/00207721.2019.1626930

[6] F. Jia, F. Cao, and X. He: Adaptive fault-tolerant tracking control for uncertain nonlinear systems with unknown control directions and limited resolution. IEEE Trans. Syst. Man Cybernet. *53* (2022), 1813–1825. DOI: 10.1109/TSMC.2022.3207903.

[7] J. Kalina, P. Vidnerová, and P. Janáček: Highly robust training of regularized radial basis function networks. Kybernetika *60* (2024), 38–59. DOI: 10.14736/kyb-2024-1-0038

[8] M. Krstic, P. V. Kokotovic, and I. Kanellakopoulos: Nonlinear and Adaptive Control Design. John Wiley and Sons, Inc., New York 1995.

[9] M. Li, Y. Chen, and Y. Liu: Adaptive disturbance observer-based event-triggered fuzzy control for nonlinear system. Inform. Sci. *575* (2021), 485–498. DOI: 10.1016/j.ins.2021.06.055

[10] W. Liu and P. Li: Disturbance observer-based fault-tolerant adaptive control for nonlinearly parameterized systems. IEEE Trans. Ind. Electron. *66* (2019), 8681–8691. DOI: 10.1109/TIE.2018.2889634

[11] W. Liu, Q. Ma, Y. Lu, and S. Xu: Adaptive fixed-time event-triggered fuzzy control for time-delay nonlinear systems with disturbances and quantization. IEEE Trans. Fuzzy Syst. *31* (2023), 2848–2860. DOI: 10.1109/TFUZZ.2023.3238410

[12] W. Liu, Q. Ma, and S. Xu: Anti-disturbance fault-tolerant adaptive output feedback control for uncertain nonlinear systems with disturbance observer. IEEE Trans. Syst. Man Cyb. *55* (2025), 2987–2997. DOI: 10.1109/TSMC.2025.3538872

[13] W. Liu, W. Tang, H. Zhao, S. Xu, and J. H. Park: Combined disturbance observer-based fuzzy finite-time preassigned performance control for state-constrained nonlinear systems. Fuzzy Set. Syst. *508* (2025), 109321. DOI: 10.1016/j.fss.2025.109321

[14] Z. G. Liu, Y. P. Tian, and Z. Y. Sun: An adaptive homogeneous domination method to time-varying control of nonlinear systems. Int. J. Robust Nonlin. *32* (2022), 527–540. DOI: 10.1002/rnc.5806

[15] L. Liu, S. Xu, X. J. Xie, B. Xiao: Observer-based decentralized control of large-scale stochastic high-order feedforward systems with multi time delays. J. Franklin Inst. *356* (2019), 9627–9645. DOI: 10.1016/j.jfranklin.2018.11.058

[16] D. G. Nguyen, D. T. Tran, and K. K. Ahn: Disturbance observer-based chattering-attenuated terminal sliding mode control for nonlinear systems subject to matched and mismatched disturbances. Appl. Sci. *11* (2021), 8158. DOI: 10.3390/app11178158

[17] A. Razzaghian, R. Kardehi Moghaddam, and N. Pariz: Disturbance observer-based fractional-order nonlinear sliding mode control for a class of fractional-order systems with matched and mismatched disturbances. Int. J. Dyn. Control *9* (2021), 671–678. DOI: 10.1007/s40435-020-00691-2

[18] H. R. Shafei, M. Bahrami, and H. A. Talebi: Disturbance observer-based two-layer control strategy design to deal with both matched and mismatched uncertainties. Int. J. Robust Nonlin. *31* (2021), 1640–1656. DOI: 10.1002/rnc.5356

[19] Y. Shen and L. Lin: Adaptive output feedback stabilization for nonlinear systems with unknown polynomial-of-output growth rate and sensor uncertainty. Kybernetika *58* (2022), 637–660. DOI: 10.14736/kyb-2022-4-0637

[20] Y. Shen, C. Ma, C. Zhao, and Z. Wu: Neural network-based fault diagnosis and fault-tolerant control for nonlinear systems with output measurement noise. Kybernetika *60* (2024), 244–270. DOI: 10.14736/kyb-2024-2-0244

[21] Z. Song and P. Li: Fixed-time adaptive command-filter-based event-triggered control of constrained switched nonlinear systems with unmodeled dynamics. Kybernetika *61* (2025), 32–57. DOI: 10.14736/kyb-2025-1-0032

[22] X. Su, C. L. P. Chen, and Z. Liu: Adaptive fuzzy control for uncertain nonlinear systems subject to full state constraints and actuator faults. Inform. Sci. *581* (2021), 553–566. DOI: 10.1016/j.ins.2021.09.055

[23] H. Sun and L. Guo: Neural network-based DOBC for a class of nonlinear systems with unmatched disturbances. IEEE Trans. Neur. Net. Lear. *28* (2016), 482–489. DOI: 10.1109/TNNLS.2015.2511450

[24] H. Sun, S. Li, J. Yang, and W. X. Zheng: Global output regulation for strict-feedback nonlinear systems with mismatched nonvanishing disturbances. Int. J. Robust Nonlin. *25* (2015), 2631–2645. DOI: 10.1002/rnc.3216

[25] Y. Wang, X. Zhan, X. Li, Y. Jiang, X. Tang, and Y. Wang: Finite-time disturbance observer-based sliding mode control for a vehicle platoon subject to mismatched disturbance. Appl. Sci. *15* (2025), 6327. DOI: 10.3390/app15116327

[26] X. Xu and Z. Zeng: Homogeneous domination-based composite adaptive control strategy for perturbed chain of integrators with mismatched disturbances. Nonlinear Dynam. *112* (2024), 15399–15411. DOI: 10.1007/s11071-024-09837-9

[27] T. Yang, N. Sun, and Y. Fang: Adaptive fuzzy control for a class of MIMO underactuated systems with plant uncertainties and actuator deadzones: Design and experiments. IEEE Trans. Cybernet. *52* (2021), 8213–8226. DOI: 10.1109/TCYB.2021.3050475

[28] S. H. Yang, Z. Y. Sun, Z. Wang, and T. Li: A new approach to global stabilization of high-order time-delay uncertain nonlinear systems via time-varying feedback and homogeneous domination. J. Franklin Inst. *355* (2018), 6469–6492. DOI: 10.1016/j.jfranklin.2018.05.063

[29] Y. Yang, J. Zhang, M. Huang, and X. Tan: Disturbance observer-based event-triggered control of switched positive systems. IEEE T. Circuits – II *71* (2023), 1191–1195. DOI: 10.1109/TCSII.2023.3325160

[30] C. Zhang, J. Yang, and S. Li: Homogeneous active disturbance attenuation for a perturbed chain of integrators. IFAC-PapersOnLine *49* (2016), 534–539. DOI: 10.1016/j.ifacol.2016.10.220

[31] F. Zhou, Y. Shen, and Z. Wu: Non-fragile observers design for nonlinear systems with unknown Lipschitz constant. Kybernetika *60* (2024), 475–491. DOI: 10.14736/kyb-2024-4-0475

*Chengcheng Wang, School of Automation, Hangzhou Dianzi University, Hangzhou 310018, Zhejiang. P. R. China.*
*e-mail: ccwang@hdu.edu.cn*

*Xianglei Jia, Corresponding author. School of Automation, Hangzhou Dianzi University, Hangzhou 310018, Zhejiang. P. R. China.*
*e-mail: jiaxianglei@126.com*

*Chengdi Xiang, School of Automation, Hangzhou Dianzi University, Hangzhou 310018, Zhejiang. P. R. China.*
*e-mail: xcd@hdu.edu.cn*

*Yingying Han, School of Mathematics, Hangzhou Normal University, Hangzhou 311121, Zhejiang. P. R. China.*
*e-mail: yyhan0826@126.com*